Biogeosciences
Discussions

EGU
Open Access

1   **Programmed cell death in diazotrophs and the fate of organic**

2   **matter in the Western Tropical South Pacific Ocean during**

3   **the OUTPACE cruise**

4

5   Dina Spungin[1], Natalia Belkin[1], Rachel A. Foster[2], Marcus Stenegren[2], Andrea Caputo[2],

6   Mireille Pujo-Pay[3], Nathalie Leblond[4], Cecile Dupouy[4], Sophie Bonnet[5], Ilana Berman-

7   Frank[1]

8

9   [1] The Mina and Everard Goodman Faculty of Life Sciences, Bar-Ilan University, Ramat-Gan, Israel.

10 [2] Stockholm University, Department of Ecology, Environment and Plant Sciences. Stockholm, Sweden.

11 [3] Laboratoire d'Océanographie Microbienne – UMR 7321, CNRS - Sorbonne Universités, UPMC Univ Paris

12 06, Observatoire Océanologique, 66650 Banyuls-sur-mer, France.

13 [4] Observatoire Océanologique de Villefranche, Laboratoire d'Océanographie de Villefranche, UMR 7093,

14 Villefranche-surmer, France.

15 [5] Aix-Marseille Univ., Univ. Toulon, CNRS/INSU, IRD, UM 110, Mediterranean Institute of Oceanography

16 (MIO) UM 110, 13288, Noumea, New Caledonia.

17

18 *Correspondence to*: Ilana Berman-Frank (Ilana.Berman-Frank@biu.ac.il)

19

20

21

22

23

24

25

26

Biogeosciences
Discussions

EGU
Open Access

27   **Abstract**

28   The fate of diazotroph (N_2 fixers) derived carbon (C) and nitrogen (N) and their contribution to vertical

29   export of C and N in the Western Tropical South Pacific Ocean was studied in OUTPACE (Oligotrophy

30   to UlTra-oligotrophy PACific Experiment). Our specific objective during OUTPACE was to determine

31   whether autocatalytic programmed cell death (PCD) is an important mechanism affecting diazotroph

32   mortality and a factor regulating the vertical flux of organic matter and thus the fate of the blooms. We

33   sampled at three long duration (LD) stations of 5 days each (LDA, LDB, and LDC) where drifting

34   sediment traps were deployed at 150, 325 and 500 m depth. LDA and LDB were characterized by high

35   chlorophyll a (Chl a) concentrations (0.2-0.6 µg L^{-1}) and dominated by dense biomass of *Trichodesmium*

36   as well as UCYN-B and diatom-diazotroph associations (*Rhizosolenia* with *Richelia*-detected by

37   microscopy and het-1 *nifH* copies). Station LDC was located at an ultra-oligotrophic area of the South

38   Pacific gyre with extremely low Chl a concentration (~ 0.02 µg L^{-1}) with limited biomass of diazotrophs

39   predominantly the unicellular UCYN-B. Our measurements of biomass from LDA and LDB yielded

40   high activities of caspase-like and metacaspase proteases that are indicative of PCD in *Trichodesmium*

41   and other phytoplankton. Metacaspase activity, reported here for the first time from oceanic populations,

42   was highest at the surface of both LDA and LDB, where we also obtained high concentrations of

43   transparent exopolymeric particles (TEP). TEP was negatively correlated with dissolved inorganic

44   phosphorus and positively coupled to both the DOC and POC pools reflecting the typically high

45   production of TEP under nutrient stress and its role as a source of sticky carbon facilitating aggregation

46   and rapid vertical sinking. Evidence for bloom decline was observed at both LDA and LDB. However,

47   the physiological status and rates of decline of the blooms differed between the stations, influencing the

48   amount of accumulated diazotrophic organic matter and mass flux observed in the traps during our

49   experimental time frame. At LDA sediment traps contained the greatest export of particulate matter and

50   significant numbers of both intact and decaying *Trichodesmium,* UCYN-B, and het-1 compared to LDB

51   where the bloom decline began only 2 days prior to leaving the station and to LDC where no evidence

52   for bloom decline was seen. Substantiating previous findings from laboratory cultures linking PCD to

53   carbon export in *Trichodesmium*, our results from OUTPACE indicate that induction of PCD by nutrient

54   limitation in high biomass blooms such as *Trichodesmium* or diatom-diazotroph associations combined

55   with high TEP production facilitates cellular aggregation and bloom termination, and expedites vertical

56   flux to depth.

57

58

59

60

61

62

63

64

1. Introduction

The efficiency of the biological pump, essential in the transfer and sequestration of carbon to the deep ocean, depends on the balance between growth (production) and death. Moreover, the manner in which marine organisms die may ultimately determine the flow of fixed organic matter within the aquatic environment and whether organic matter is incorporated into higher trophic levels, recycled within the microbial loop sustaining subsequent production, or sink out (and exported) to depth.

Important contributors to the biological pump are N_2 fixing (diazotrophic) prokaryotic organisms whose ability to fix atmospheric N_2 confers an inherent advantage in the nitrogen-limited surface waters of many regions. The oligotrophic waters of the Western Tropical South Pacific (WTSP) have been characterized by some of the highest recorded rates of N_2 fixation (151-700 μmol N m^{-2} d^{-1}) (Garcia et al., 2007;Bonnet et al., 2005), and can reach up to 1200 μmol N m^{-2} d^{-1} (Bonnet et al., 2017b). These rates of N_2 fixation are accompanied with diazotrophic communities comprised of unicellular cyanobacteria lineages (UCYNA, B and C), diatom-diazotroph associations such as *Richelia* associated with *Rhizosolenia,* and diverse heterotrophic bacteria such as alpha and γ-protobacteria. The most conspicuous of all diazotrophs, and predominating in terms of biomass, is the filamentous bloom-forming cyanobacteria *Trichodesmium* forming massive surface blooms that supply ~ 60-80 Tg N yr^{-1} of the 100-200 Tg N yr^{-1} of the estimated marine N_2 fixation (Capone et al., 1997;Carpenter et al., 2004) with a large fraction fixed in the South West tropical Pacific (Dupouy et al., 2000;Dupouy et al., 2011;Tenorio et al., in review) that may, based- on NanoSIMS cell-specific measurements, contribute up to ~ 80 % of bulk N_2 fixation rates in the WTSP (Bonnet et al., 2017a).

How *Trichodesmium* or other diazotrophic blooms form and develop has been intensely investigated while little data is found regarding the fate of blooms. *Trichodesmium* blooms often collapse within 3-5 days, with mortality rates paralleling bloom development rates (Rodier and Le Borgne, 2008;Rodier and Le Borgne, 2010;Bergman et al., 2012). Cell mortality can occur due to grazing (O'Neil, 1998), viral lysis (Hewson et al., 2004;Ohki, 1999), and/or programmed cell death (PCD) an autocatalytic genetically controlled death (Berman-Frank et al., 2004). PCD is induced in response to oxidative and nutrient stress, as has been documented in both laboratory and natural populations of *Trichodesmum* (Berman-Frank et al., 2004;Berman-Frank et al., 2007) and in other phytoplankton (Bidle, 2015). The cellular and morphological features of PCD in *Trichodesmium*, include elevated gene expression and activity of metacaspases and caspase like-proteins important for initiation and execution of PCD; increased production of transparent exopolymeric particles (TEP) whose sticky matrix augments cell and particle aggregation; loss of buoyancy by gas-vesicle degradation resulting in rapid sinking rates (Bar-Zeev et al., 2013;Berman-Frank et al., 2004).

Simulating PCD in laboratory cultures of *Trichodesmium* in 2 m water columns (Bar-Zeev et al., 2013) led to a collapse of the *Trichodesmium* biomass and to greatly enhanced sinking of large

Biogeosciences

Discussions

Open Access

EGU

100 aggregates reaching rates of up to ~ 200 m d^{-1} that efficiently exported particulate organic carbon

101 (POC) and particulate organic nitrogen (PON) to the bottom of the water column. Although the

102 sinking rates and degree of export from this model system could not be extrapolated to the ocean, this

103 study mechanistically linked autocatalytic PCD and bloom collapse to quantitative C and N export

104 fluxes, suggesting that PCD may have an impact on the biological pump efficiency in the oceans (Bar-

105 Zeev et al., 2013).

106   We further examined this issue in the open ocean and investigated the cellular processes mediating

107 *Trichodesmium* mortality in a large surface bloom from the New Caledonian lagoon (Spungin et al.,

108 2016). Nutrient stress induced a PCD mediated crash of the *Trichodesmium* bloom. The filaments and

109 colonies were characterized by upregulated expression of metacaspase genes, downregulated

110 expression of gas-vesicle genes, enhanced TEP production, and aggregation of the biomass (Spungin

111 et al., 2016). However, due to experimental conditions we could not measure the subsequent export

112 and vertical flux of the dying biomass in the open ocean. Moreover, while the existence and role of

113 PCD and its mediation of biogeochemical cycling of organic matter has been investigated in

114 *Trichodesmium*, scarce information exists about PCD and other mortality pathways of other common

115 marine diazotrophs.

116   The OUTPACE (Oligotrophy to UlTra-oligotrophy PACific Experiment) cruise was conducted

117 from 18 February to 3 April 2015 along a west to east gradient from the oligotrophic area north of

118 New Caledonia to the ultraoligotrophic western South Pacific gyre (French Polynesia). The goal of the

119 OUTPACE experiment was to study the diazotrophic blooms and their fate within the oligotrophic

120 ocean in the Western Tropical South Pacific Ocean (Moutin et al., 2017). Our specific objective was to

121 determine whether PCD was an important mechanism affecting diazotroph mortality and a factor

122 regulating the fate of the blooms by mediation of vertical flux of organic matter. The strategy and

123 experimental approach of the OUTPACE transect enabled sampling at three long duration (LD)

124 stations of 5 days each (referred to as stations LDA, LDB, and LDC) and provided 5-day snapshots

125 into diazotroph physiology, dynamics, and mortality processes. We specifically probed for the

126 induction and operation of PCD and examined the relationship of PCD to the fate of organic matter

127 and vertical flux from diazotrophs by the deployment of 3 sediment traps at 150, 325 and 500 m

128 depths.

129

130

131

132

133

Biogeosciences
Discussions

Open Access

EGU

134 **2. Methods**

135
136 **2.1. Sampling site and sampling conditions**

137   Sampling was conducted on a transect during austral summer (18 Feb-5 Apr, 2015), on board of

138 the R/V L'Atalante (Moutin et al., 2017). Samples were collected from three long duration stations

139 (LD-A, LD-B and LD-C) where the ship remained for 5 days at each location and 15 short duration

140 (SD1-15) stations (approximately eight hours duration). The cruise transect was divided into two

141 geographic regions. The first region (Melanesian archipelago, MA) included SD1-12, LDA and LDB

142 stations (160º E-178º E and 170º-175º W). The second region (subtropical gyre, GY) included SD 13-

143 15 and LDC stations (160º W-169º W).

144
145 **2.2. Chlorophyll *a***

146   Samples for determination of (Chl *a*) concentrations were collected by filtering 550 ml sea water

147 on GF/F filters (Whatman, UK). Filters were frozen and stored in liquid nitrogen, Chl *a* was extracted

148 in Methanol and measured fluorometrically (Turner Designs Trilogy Optical kit) (Le Bouteiller et al.,

149 1992). Satellite derived surface Chl *a* concentrations at the LD stations were used from before and

150 after the cruise sampling at the LD stations. Satellite Chl *a* data are added as supplementary video files

151 (Supplementary videos S1, S2, S3).

152
153 **2.3. Caspase and metacaspase activities**

154   Biomass was collected on 25 mm, 0.2 µm pore-size polycarbonate filters and resuspended in 0.6-1

155 ml Lauber buffer [50 mM HEPES (pH 7.3), 100 mM NaCl, 10 % sucrose, 0.1 % (3-cholamidopropyl)-

156 dimethylammonio-1-propanesulfonate, and 10 mM dithiothreitol] and sonicated on ice (four cycles of

157 30 seconds each) using an ultracell disruptor (Sonic Dismembrator, Fisher Scientific, Waltham, MA,

158 USA). Cell extracts were centrifuged (10,000 x g, 2 min, room temperature), and the supernatant was

159 collected for caspase and metacaspase activity measurements. Caspase specific activity (normalized to

160 total protein concentration) was determined by measuring the kinetics of cleavage for the fluorogenic

161 caspase substrate (Z-IETD-AFC) at a 50 mM final concentration (using Ex 400 nm, Em 505 nm;

162 Synergy4 BioTek, Winooski, VT, USA), as previously described in Bar-Zeev et al. (2013).

163 Metacaspase specific activity (normalized to total protein concentration) was determined by measuring

164 the kinetics of cleavage for the fluorogenic metacaspase substrate (Av-Val-Arg-Pro-Arg-AMC),

165 (Klemenčič et al., 2015;Tsiatsiani et al., 2011) at a 50 mM final concentration (using Ex 380 nm, Em

166 460 nm; Synergy4 BioTek, Winooski, VT, USA) (Klemenčič et al., 2015;Tsiatsiani et al., 2011).

167 Relative fluorescence units were converted to protein-normalized substrate cleavage rates using AFC

168 and AMC standards (Sigma) for caspase and metacaspase activities, respectively. Total protein

169 concentrations were determined by Pierce™ BCA protein assay kit (Thermo Scientific product

170 #23225).

Biogeosciences

Discussions

Open Access

EGU

2.4. Phosphate analysis

Seawater for PO_4^{3-} analysis were collected in 20 mL high-density polyethylene HCL-rinsed bottles and poisoned with $HgCl_2$ to a final concentration of 20 µg L^{-1}, stored at 4 °C until analysis. Phosphate (PO_4^{3-}, DIP) was determined by a standard colorimetric technique using a segmented flow analyzer according to Aminot and Kérouel (2007) on a SEAL Analytical AA3 HR system 20 (SEAL Analytica, Serblabo Technologies, Entraigues Sur La Sorgue, France). Quantification limits for phosphate were 0.05 µmol L^{-1}.

2.5. Particulate organic carbon (POC) and nitrogen (PON)

Samples were filtered through pre-combusted (4 h, 450 ºC) GF/F filters (Whatman GF/F, 25 mm), dried overnight at 60 ºC and stored in a desiccator until further analysis. POC and PON were determined using a CHN analyzer Perkin Elmer (Waltham, MA, USA) 2400 Series II CHNS/O Elemental Analyzer after carbonate removal from the filters using overnight fuming with concentrated HCl vapor.

2.6. Dissolved organic carbon (DOC) and Total organic carbon (TOC)

Samples were collected from the Niskin bottles in combusted glass bottles and were immediately filtered through 2 precombusted (24 h, 450 ºC) glass fiber filters (Whatman GF/F, 25 mm). Filtered samples were collected into glass precombusted ampoules that where sealed immediately after filtration. Samples were acidified with Orthophosphoric acid (H_3PO_4) and analyzed by high temperature catalytic oxidation (HTCO) (Sugimura and Suzuki, 1988;Cauwet, 1994) on a Shimadzu TOC-L analyzer. TOC was determined as POC+DOC.

2.7. Transparent exopolymeric particles (TEP)

Water samples (100 mL) were gently (< 150 mbar) filtered through a 0.45 µm polycarbonate filter (GE Water & Process Technologies). Filters were then stained with a solution of 0.02 % Alcian blue (AB) and 0.06 % acetic acid (pH of 2.5), and the excess dye was removed by a quick deionized water rinse. Filters were then immersed in sulfuric acid (80 %) for 2 h, and the absorbance (787 nm) was measured spectrophotometrically (CARY 100, Varian). AB was calibrated using a purified polysaccharide gum xanthan (GX) (Passow and Alldredge, 1995). TEP concentrations (µg GX equivalents L^{-1}) were measured according to Passow and Alldredge (1995). To estimate the role of TEP in C cycling, the total amount of TEP-C was calculated using the TEP concentrations at each depth, and the conversion of GX equivalents to carbon applying the revised factor of 0.63 based on empirical experiments from both natural samples from different oceanic areas and phytoplankton cultures (Engel, 2004).

6

2.8. Diazotrophic abundance

The full description of DNA extraction, primer design and qPCR analyses are described in detail in this issue (Stenegren et al., 2017). Briefly, 2.5 L of water from 6-7 depths with surface irradiance light intensity (100, 75, 54, 36, 10, 1, and 0.1 %) were sampled and filtered onto a 25 mm diameter Supor filter (Pall Corporation, PallNorden, AB Lund Sweden) with a pore size 0.2 μm filters. Filters were stored frozen in pre-sterilized bead beater tubes (Biospec Bartlesville Ok, USA) containing 30 mL of 0.1 mm and 0.5 mm glass bead mixture. DNA was extracted from the filters using a modified protocol of the Qiagen DNAeasy plant kit (Moisander et al., 2008) and eluted in 70 μL. With the re-eluted DNA extracts ready, samples were analyzed using the qPCR instrument StepOnePlus (Applied Biosystems) and fast mode. Previously designed TaqMAN assays and oligonucleotides and standards were prepared in advance and followed previously described methods for the following cyanobacterial diazotrophs: *Trichodesmium*, UCYN-A1, UCYN-A2, UCYN-B, *Richelia* symbionts of diatoms (het-1, het-2, het-3) (Stenegren et al., 2017;Church et al., 2005;Foster et al., 2007;Moisander et al., 2010;Thompson et al., 2012). .

2.9. Microscopy

Samples for microscopy were collected in parallel from the same depth profiles for nucleic acid as described in Stenegren et al. (2017). Briefly, 2 profiles were collected on day 1 and 3 at each LD station and immediately filtered onto a 47 mm diameter Poretics (Millipore, Merck Millipore, Solna, Sweden) membrane filter with a pore size of 5 μm using a peristaltic pump. After filtration samples were fixed with a 1 % paraformaldehyde (v/v) for 30 min. prior to storing at -20 °C. The filters were later mounted onto an oversized slide, and examined under an Olympus BX60 microscope equipped with blue (460-490 nm) and green (545-580 nm) excitation wavelengths. Three areas (0.94 mm^2) per filter were counted separately and values were averaged. When abundances were low, the entire filter (area=1734 mm^2) was observed and cells enumerated. Due to poor fluorescence, only *Trichodesmium* colonies and free-filaments could be accurately enumerated by microscopy, and in addition the larger cell diameter *Trichodesmium* (*Katagynemene pelagicum*) was counted separately as these were often present albeit at lower densities. Other cyanobacterial diazotrophs (e.g. *Crocosphaera* watsonii-like cells, the *Richelia* symbionts of diatoms were present but with poor fluorescence and could only be qualitatively noted.

2.10. Particulate matter from sediment traps

Particulate matter export was quantified with three PPS5 sediment traps (1 m^2 surface collection, Technicap, France) deployed for 5 days at 150, 330 and 520 m at each LD station. Particle export was recovered in polyethylene flasks screwed on a rotary disk which allowed flasks to be changed automatically every 24-h to obtain a daily material recovery. The flasks were previously filled with a

240 buffered solution of formaldehyde (final conc. 2 %) and were stored at 4 °C until analysis to prevent

241 degradation of the collected material. The flask corresponding to the fifth day of sampling on the

242 rotary disk was not filled with formaldehyde to collect 'fresh particulate matter' for further diazotroph

243 quantification. Exported particulate matter was weighed and analyzed on EA-IRMS (Integra2, Sercon

244 Ltd) to quantify exported PC and PN.

245 **2.11.   Diazotroph abundance in the traps**

246   Triplicate aliquots of 2-4 mL from the flask dedicated for diazotroph quantification were filtered

247 onto 0.2 μm Supor filters, flash frozen in liquid nitrogen and stored in at -80 °C until analyses. Nucleic

248 acids were extracted from the filters as described in Moisander et al. (2008) with a 30 second

249 reduction in the agitation step in a Fast Prep cell disruptor (Thermo, Model FP120; Qbiogene, Inc.

250 Cedex, Frame) and an elution volume of 70 μl. Diazotroph abundance for *Trichodesmium* spp.,

251 UCYN-B, UCYN-A1, het-1, and het-2 were quantified by qPCR analyses on the *nifH* gene using

252 previously described oligonucleotides and assays (Foster et al., 2007;Church et al., 2005). The qPCR

253 was conducted in a StepOnePlus system (applied Biosystems, Life Technologies, Stockholm Sweden)

254 with the following parameters: 50 °C for 2 min, 95°C for 10 min, and 45 cycles of 95°C for 15s

255 followed by 60°C for 1 min. Gene copy numbers were calculated from the mean cycle threshold (Ct)

256 value of three replicates and the standard curve for the appropriate primer and probe set. For each

257 primer and probe set, duplicate standard curves were made from 10-fold dilution series ranging from

258 108 to 1 gene copies per reaction. The standard curves were made from linearized plasmids of the

259 target *nifH* or from synthesized gBLocks gene fragments (IDT technologies, Cralville, Iowa USA).

260 Regression analyses of the results (number of cycles=Ct) of the standard curves were analyzed in

261 Excel. 2 μl of 5 KDa filtered nuclease free water was used for the no template controls (NTCs). No

262 *nifH* copies were detected for any target in the NTC. In some samples only 1 or 2 of the 3 replicates

263 produced an amplification signal; these were noted as detectable but not quantifiable (dnq). A 4th

264 replicate was used to estimate the reaction efficiency for the *Trichodesmium* and UCYN-B targets as

265 previously described in (Short et al., 2004). Seven and two samples were below 95 % in reaction

266 efficiency for *Trichodesmium* and UCYN-B, respectively. The detection limit for the qPCR assays is

267 1-10 copies.

268 **2.12.   Statistics**

269   A Pearson correlation coefficient test was applied to examine the association between two

270 variables after linear regressions or log transformation of the data. Statistical analyses were carried out

271 with XLSTAT, a Microsoft Office Excel based software.

272

273

274 **3. Results and discussion**
275 **3.1. Diazotrophic characteristics and abundance in the LD stations**

276   The sampling strategy of the transect was planned so that changes in abundance and fate of
277 diazotrophs could be followed in "long duration" stations where measurements were taken from the
278 same water mass (and location) over 5 days and drifting sediment traps were deployed (Moutin et al.,
279 2017). Although rates for the different parameters were obtained for 5 days, this period is still a
280 "snapshot" in time with the processes measured influenced by preceding events and also continuing
281 after the ship departed. Specifically, production of photosynthetic biomass (as determined from
282 satellite-derived Chl a) and development of surface phytoplankton blooms, including cyanobacterial
283 diazotrophs, displayed specific characteristics for each of the long duration stations. We first examined
284 the satellite-derived surface Chl a concentrations by looking at changes around the long duration (LD)
285 stations before and after our 5 day sampling at each station [daily surface Chl a (mg m^{-3})]
286 (Supplementary videos S1, S2, S3).

287   At LDA, satellite data confirmed high concentrations of Chl a indicative of intense surface blooms
288 ($\sim$ 0.55 µg L^{-1}) between 8.02.15 to 19.02.15 which began to gradually decline with over 60 % Chl a
289 reduction until day 1 at the station (Supplementary video S1, Fig. 1a). By the time we reached LDA on
290 25.02.15 (day 1) Chl a concentrations averaged $\sim$ 0.2 µg L^{-1} Chl a at the surface (Fig. 1a) and
291 remained steady for the next 5 days with Chl a values of 0.23 µg L^{-1} measured on day 5 (Fig 1a).
292 When looking for biomass at depth the DCM recorded at $\sim$ 80 m depth was characterized by Chl a
293 concentrations increasing from 0.34 to 0.48 µg L^{-1} between day 3 and 5 respectively (Fig. 1d). While
294 the Chl a values of the surface biomass decreased for approximately one week prior to our sampling at
295 station, the Chl a concentrations measured at depth increased during the corresponding time.

296   In contrast to LDA, the satellite data from LDB confirmed the presence of a surface bloom/s for
297 over one month prior to our arrival at the station on 15.3.15 (day 1) (Supplementary video S2, Fig.
298 1b). This bloom was characterized by high surface Chl a concentrations ($\sim$ 0.6 µg L^{-1}, Supplementary
299 video S2) and on day 1 at the station surface Chl a was 0.58 µg L^{-1} (Fig. 1b). Surface Chl a then
300 decreased over the next days at the station with a 50 % reduction of Chl a concentration from the sea
301 surface (5m) on day 5 (0.35 µg L^{-1}), (Fig. 1e). Thus, it appears that our 5 sampling days at LDB were
302 tracking a surface bloom that had only began to decline after day 3 and continued to decrease ($\sim$ 0.1
303 µg L^{-1}) also after we have left (Fig.1b). On day 1 of sampling, the DCM at LDB was relatively
304 shallow, at 40 m with Chl a values of 0.5 µg L^{-1}. By day 5 the DCM had deepened to 80 m (de Verneil
305 et al., 2017).

306   LDC was located in a region of extreme oligotrophy within the Cook Islands territorial waters
307 (GY waters). This station was characterized historically ($\sim$ 4 weeks before arrival) by extremely low
308 Chl a concentrations at the surface ($\sim$ 0.02 µg L^{-1}, Supplementary video S3) that were an order of

309   magnitude lower than average Chl *a* measured at LDA and LDB. These values remained low with no

310   significant variability for the 5 days at station or later (Fig. 1f) (Supplementary video S3, Fig. 1c).

311   Similar to the results from LDA, the DCM at LDC was found near the bottom of the photic layer at ~

312   135 m, with Chl *a* concentrations about 10-fold higher than those measured at surface with ~ 0.2 µg

313   L^{-1} (Fig. 1f).

314   Chl *a* is an indirect proxy of photosynthetic biomass and we thus needed to ascertain who the

315   dominant players (specifically targeting diazotrophic populations) were at each of the LD stations.

316   Moreover, At LDA and LDB diazotrophic composition and abundance as determined by qPCR

317   analysis were quite similar. At LDA *Trichodesmium* was the most abundant diazotroph, ranging

318   between $6x10^4$ -$1x10^6$ *nifH* copies L^{-1} in the upper water column (0-70 m). UCYN-B (genetically

319   identical to *Crocosphaera watsonii*) co-occurred with *Trichodesmium* between 35 and 70 m, and het1

320   specifically identifying the diatom-diazotroph association (DDA) between the diatom *Rhizosolenia*

321   and the heterocystous diazotroph *Richelia,* was observed only at the surface waters at 4 m. UCYN-B

322   and het-1 abundances were relatively lower than *Trichodesmium* abundances with $2x10^2$ *nifH* copies

323   L^{-1} and $3x10^3$ *nifH* copies L^{-1} respectively (Stenegren et al., 2017). Microscopic observations from

324   LDA indicated that near the surface *Rhizosolenia* populations were already showing signs of decay

325   since the silicified cell-wall frustules were broken and free filaments of *Richelia* were observed (Fig.

326   2e-f) (Stenegren et al., 2017). DDAs are significant N$_2$ fixers in the oligotrophic oceans. Although

327   their abundance in the WTSP is usually low, they are common and highly abundant in the New

328   Caledonian lagoon significantly impacting C sequestration and rapid sinking (Turk-Kubo et al., 2015).

329   At LDB, *Trichodesmium* was also the most abundant diazotroph with *nifH* copies L^{-1} ranging

330   between $1x10^4$-$5x10^5$ within the top 60 m (Stenegren et al., 2017). Microscopical analyses confirmed

331   high abundance of free filaments of *Trichodesmium* at LDB, while colonies were rarely observed

332   (Stenegren et al., 2017). Observations of poor cell integrity were reported for most collected samples,

333   with filaments at various stages of degradation and colonies under possible stress (Fig. 2a-d). In

334   addition to *Trichodesmium*, UCYN-B was the second most abundant diazotroph ranging between

335    $1x10^2$ and $2x10^3$ *nifH* copies L^{-1}. Other unicellular diazotrophs of the UCYN groups (UCYN-A1 and

336   UCYN-A2) were the least detected diazotrophs (Stenegren et al., 2017). Of the three heterocystous

337   cyanobacterial symbiont lineages (het-1, het-2, het-3), het-1 was the most dominant ($1x10^1$-$4x10^3$ *nifH*

338   copies L^{-1}), (Stenegren et al., 2017). Microscopic analyses from LDB demonstrated the co-occurrence

339   of degrading diatom cells, mainly belonging to *Rhizosolenia* (Stenegren et al., 2017) (Fig. 2e-f).

340   In contrast to LDA and LDB, at LDC, the highest *nifH* copy numbers (up to $6x10^5$ *nifH* copies L^{-1} at

341   60 m depth were from the unicellular diazotrophs UCYN-B (Stenegren et al., 2017) *Trichodemsium*

342   was only detected at 60 m and with very low copy numbers of *nifH* (~$7x10^2$ *nifH* copies L^{-1})

343   (Stenegren et al., 2017).

344   Corresponding to the physiological status of the bloom, higher N_2 fixation rates (45.0 nmol N L^{-1}

345   d^{-1}) were measured in the surface waters (5m) of LDB in comparison with those measured at LDA and

346   LDC (19.3 nmol N L^{-1} d^{-1} in LDA and below the detection limit at LDC at 5m), (Caffin et al., 2017).

347

348   **3.2. Diazotrophic bloom demise in the LD stations**

349   Of the 3 long duration stations we examined, LDA and LDB had a higher biomass of diazotrophs

350   during the 5 days of sampling and as shown (section 3.1). Furthermore, while our analyses examining

351   bloom dynamics show these stations experiencing different stages of decline from the satellite-derived

352   Chl *a* concentrations, both LDA and LDB were still characterized by high (and visible to the eye at

353   surface) biomass on the first sampling day at each station (day 1) as determined by qPCR and

354   microscopy (Stenegren et al., this issue). This is different from LDC where biomass was extremely

355   limited, and no clear evidence was obtained for any specific bloom or bloom demise. We therefore

356   show results mostly from LDA and LDB and focus specifically on the evidence for PCD and

357   diazotroph decline in areas with high biomass and surface blooms.

358   Although the mortality of phytoplankton at sea can be difficult to discern as it results from

359   several processes (grazing, viral lysis, PCD), not necessarily acting independently of one another, we

360   here focused on evidence for PCD and whether the influence of zooplankton grazing on the

361   diazotrophs and especially on *Trichodesmium* at LDA and LDB impacted bloom dynamics. At LDA

362   and LDB total zooplankton population was generally low. Total zooplankton population at LDA

363   ranged between 911-1900 individuals m^{-3} and in LDB between 1209-2188 individuals m^{-3} on day 1

364   and day 5 respectively. *Trichodesmium* is toxic and inedible to most zooplankton excluding three

365   species of harpacticoid zooplankton (O'Neil and Roman, 1994). During our sampling days at these

366   stations, *Macrosettella gracilis* a specific grazer of *Trichodesmium* comprised less than 1 % of the

367   total zooplankton community with another grazer *Miracia efferata* comprising less than 0.1 % of total

368   zooplankton community. *Oculosetella gracilis* was not found at these stations. The low number of

369   harpacticoid zooplankton specifically grazing on *Trichodesmium* found in the LDA and LDB station,

370   refutes the possibility that grazing caused the massive demise of the bloom. Moreover, the toxicity of

371   *Trichodesmium* to many grazers (Rodier and Le Borgne, 2008;Kerbrat et al., 2011) could critically

372   limit the amount of *Trichodesmium*-derived recycled matter within the upper mixed layer. Virus

373   abundance and activity were not enumerated in this study, so we cannot estimate their influence on

374   mortality.

375   Previous studies demonstrated that limited availability of Fe and P induce PCD in

376   *Trichodesmium*. At LDA and LDB, Fe concentrations were relatively high, possibly due to island

377   effects (de Verneil et al., 2017), that could have created favorable conditions for diazotrophs that

378   require high Fe for the energy expensive processes of N_2 fixation and photosynthesis and thus could

379   enhance the potential for increased growth rates and the formation of dense surface blooms.

380 Phosphorus availability, or lack of phosphorus, can also induce PCD (Berman-Frank et al.,

381 2004;Spungin et al., 2016). PO_4^{3-} concentrations at the surface (0-40m) of LDA and LDB stations

382 were extremely low around 0.05 µmol L^{-1} (de Verneil et al., 2017), possibly consumed by the high

383 biomass and high growth rates of the bloom causing nutrient stress and bloom mortality. PO_4^{3-}

384 concentrations observed at LDC were above the quantification limit with average values of 0.2 µmol

385 L^{-1} in the 0-150 m depths (data not shown). These limited P concentrations may curtail the extent of

386 growth, induce PCD, and pose an upper limit on biomass formation.

387   Here we compared, for the first time in oceanic populations, two PCD indices, caspase and

388 metacaspase activities, to examine the presence/operation of PCD in the predominant phytoplankton

389 (and diazotroph) populations along the transect. We specifically show the results from LDA and LDB

390 where biomass and activities were detectable. Classic caspases are absent in phytoplankton, including

391 in cyanobacteria, and are unique to metazoans and several viruses (Minina et al., 2017). In diverse

392 phytoplankton the presence of a C14 caspase domain suffices to demonstrate caspase-like proteolytic

393 activity that occurs upon PCD induction when the caspase specific substrate IETD-AFC is added.

394 Cyanobacteria and many diazotrophs do contain genes that are similar to caspases, the metacaspases-

395 cysteine proteases that share structural properties with caspases, specifically a histidine-cysteine

396 catalytic dyad in the predicted active site (Tsiatsiani et al., 2011). While the specific role and functions

397 of these genes are unknown, preliminary investigations have indicated that when PCD is induced some

398 of these genes are upregulated (Bidle and Bender, 2008;Spungin et al., 2016). Of the abundant

399 diazotrophic populations at LDA and LDB 12 metacaspases have previously been identified in

400 *Trichodesmium* (Asplund-Samuelsson et al., 2012;Asplund-Samuelsson, 2015;Jiang et al.,

401 2010;Spungin et al., 2016). Phylogenetic analysis of a wide diversity of truncated metacaspase

402 proteins, containing the conserved and characteristic caspase super family (CASc; cl00042) domain

403 structure, revealed metacaspase genes in both *Richelia* (het-1) from the diatom-diazotroph association

404 and *Crocosphaera watsonii* (a cultivated unicellular cyanobacterium) which is genetically identical to

405 the UCYN-B *nifH* sequences (Spungin et al., unpublished data).

406   We compared between metacaspase and caspase-like activities for the > 0.2 µm fraction

407 sampled assuming that the greatest activity would be due to the principle organisms contributing to the

408 biomass – i.e the diazotrophic cyanobacteria. Caspase activity and metacaspase activity were

409 specifically measured during all LD stations (days 1,3,5) at 5 depths between 0-200 m. Caspase

410 activity at the surface waters (50 m) at LDA, as determined by the cleavage of IETD-AFC substrate,

411 was between 2.3±0.1-2.8±0.1 pM hydrolyzed mg protein^{-1} on days 1 and 3 respectively (Fig. 3a). The

412 highest activity was measured on day 5 at 50 m with 5.1±0.1 pM hydrolyzed mg protein^{-1}. Similar

413 trends were obtained at LDA for metacaspase activity as measured by the cleavage of the VRPR-AMC

414 substrate, containing an Arg residue at the P1 position, specific for metacaspase cleavage, (Tsiatsiani

415 et al., 2011;Klemenčič et al., 2015). High and similar metacaspase activities were measered on days 1

Biogeosciences
Discussions

416   and 3 (50 m) with 32±4 and-35±0.2 pM hydrolyzed mg protein^{-1} respectively (Fig. 3a). The highest

417   metacaspase activity was measured on day 5 at 50 m with 59±1 pM hydrolyzed mg protein^{-1} at 50 m

418   decreasing with depth (Fig. 3b).

419   Caspase activity at LDB, was similar at all sampling days, with highest activity at the surface,

420   ranging from 3±0.1 to 4.5±0.2 pM hydrolyzed mg protein^{-1} min^{-1} at 7 m depth and then decreasing

421   with depth (Fig. 3d). At day 3 caspase activity at LDB increased at the surface with 4.5±0.2 pM

422   hydrolyzed mg protein^{-1} min^{-1} and then declined by day 5 back to 3±0.1 pM hydrolyzed mg protein^{-1}

423   min^{-1}. The decrease in activity at the surface between day 3 and 5 was accompanied by an increase in

424   caspase activity measured in the DCM between day 3 and 5 (Fig. 3d). Caspase activity at the DCM at

425   day 3 (35 m) was 1±0.4 pM hydrolyzed mg protein^{-1} min^{-1} and by day 5 increased to 3±0.1 pM

426   hydrolyzed mg protein^{-1} min^{-1} at the 70 m depth of the DCM. Thus, at LDB, caspase activity increased

427   from day 1 to 5 and with depth, with higher activities that initially were recorded at surface and then at

428   depth coupled with the decline of the bloom (Fig. 3d). Similar trends were obtained at LDB for

429   metacaspase activity with the 11.1±pM hydrolyzed mg protein^{-1} min^{-1} at the surface (7 m) on day 1. A

430   4-fold increase in activity was measured at the surface on day 3 with 40.1±5 pM hydrolyzed mg

431   protein^{-1} min^{-1} (Fig. 3e). Similar high activities were measured also on day 5 (Fig. 3e). However, the

432   increase in activity was also pronounced at depth of ~ 70 m and not only at the surface. Metacaspase

433   activity at day 5 was the highest with 40.3±0.5 and 44.6±5 pM hydrolyzed mg protein^{-1} min^{-1} at 7 and

434   70 m respectively (Fig 3e). The relatively low metacaspase activity at day 1, corresponds with the

435   physiological stage of the bloom, which we believe was just prior to enhanced mortality and death.

436   Metacaspase activity increased corresponding with the pronounced decline in Chl a from day 1 to day

437   5 (Fig. 1b).

438   Metacaspase activities were generally 10-fold higher than caspase activity rates obtained (Fig

439   3). Metacaspase and caspase activities are significantly and positively correlated at LDA and LDB

440   (r=0.8, p<0.05 and r=0.8 p<0.001 for LDA and LDB respectively) (Fig. 3c and 3f). Both findings (i.e.

441   higher metacaspase activity and tight correlation between metacaspase and caspases) were

442   demonstrated specifically in cultures and natural populations of *Trichodesmium* undergoing PCD

443   (Spungin et al., unpublished). *Trichodesmium* metacaspses are substrate specific, and activity is

444   enhanced as PCD progresses (Spungin et al. unpublished). We do not know what protein is

445   responsible for the caspase-specific activities and what drivers regulate it. Yet, the tight correlation

446   between both activities specifically for *Trichodesmium,* and here at LDA and LDB suggest that both

447   activities occur in the cell when PCD is induced. To date, we are not aware of any previous studies

448   examining metacaspase or caspase activity (or the existence of PCD) in diatom-diazotroph

449   associations such as *Rhizolsolenia* and *Richelia*.

450

3.3. TEP dynamics and carbon pools

Transparent exopoloymeric particles, that are formed both biotically and abiotically in the ocean, link between the particulate and dissolved carbon fractions and act to augment the coagulation of colloidal precursors from the dissolved organic matter and from biotic debris and to increase vertical carbon flux (Passow, 2002;Verdugo and Santschi, 2010). TEP production also increases upon PCD induction – specifically in large bloom forming organisms such as *Trichodesmium* (Berman-Frank et al., 2007;Bar-Zeev et al., 2013).

At LDA, TEP concentrations at 50 m depth were highest at day 1 with measured concentrations of 562 ± 7 µg GX L^{-1} (Table. 1) that appear to correspond with the declining physiological status of the cells that were sampled at that time (Fig. 2a-d). TEP concentrations during days 3 and 5 decreased to less than 350 µg GX L^{-1}, and it is possible that most of the TEP had been formed and sank prior to our measurements in the LDA.

At LDB, TEP concentrations at day 1 and 3 were similar with ~ 400 µg GX L^{-1} at the surface (7 m) while concentrations decreased about 2-fold with depth, averaging at 220 ± 56 and 253 ± 32 µg GX L^{-1} (35-200 m) for day 1 and 3 respectively (Fig. 4a, Table 2). A significant (> 150 %) increase in TEP concentrations was observed on day 5 compared to previous days, with TEP values of 597 ± 69 µg GX L^{-1} at the surface (7m) (Fig 4b, Table 2). Although TEP concentrations were elevated at surface, the difference in averaged TEP concentrations observed at the deeper depths (35-200 m) between day 3 (157 ± 28 µg GX L^{-1}) and day 5 (253 ± 32 GX L^{-1}) indicated that TEP from the surface was either breaking down or sinking to depth (Fig. 4a, Table 2). Our measured TEP concentrations correspond with values and trends reported from other marine environments (Engel, 2004;Bar-Zeev et al., 2009) and specifically with TEP concentrations measured from the New Caledonian lagoon (Berman-Frank et al., 2016).

TEP is produced by many phytoplankton including cyanobacteria under conditions uncoupling growth from photosynthesis (i.e. nutrient but not carbon limitation) (Berman-Frank and Dubinsky, 1999;Passow, 2002;Berman-Frank et al., 2007). Decreasing availability of dissolved nutrients such as nitrate and phosphate has been correlated with increase in TEP concentrations in both cultured phytoplankton and natural marine systems (Bar-Zeev et al., 2013;Brussaard et al., 2005;Engel et al., 2002;Urbani et al., 2005). TEP production in *Trichodesmium* is enhanced as a function of nutrient stress (Berman-Frank et al., 2007) yet, *Crocosphaera watsonii* (similar to UCYN-B) (> 4 µm cell size) also produces large amounts of extracellular polysaccharides (EPS) during exponential growth (Sohm et al., 2011).

In the New Caledonian coral lagoon TEP concentrations were negatively correlated with ambient concentrations of dissolved inorganic phosphorus (DIP) (Berman-Frank et al., 2016). Here, at LDB a significant negative correlation of TEP with DIP was also observed (Fig. 4b, $p<0.001$),

486   suggesting that lack of phosphorus set a limit to continued biomass increase and stimulated TEP

487   production in the nutrient-stressed cells. TEP production was also positively correlated with

488   metacaspase activity at all days (Fig. 4c, p<0.05) further indicating that biomass undergoing PCD

489   produced more TEP. In the diatom *Rhizosolenia setigera* TEP concentrations increased during the

490   stationary- decline phase (Fukao et al., 2010) and could also affect buoyancy. PCD in *Trichodesmium*

491   leading to elevated production of TEP and aggregation has been previously shown in *Trichodesmium*

492   cultures (Berman-Frank et al., 2007;Bar-Zeev et al., 2013) and here in oceanic populations as the

493   bloom declined (Fig. 4c) (Spungin et al., 2016).

494   TEP concentrations at LDB were positively correlated to TOC, POC, and DOC (Fig. 4d-f)

495   confirming the integral part of TEP in the cycling of carbon at this station. Assuming a carbon content

496   of 63 % (w/w), (Engel, 2004) we estimate that TEP contributes to the organic carbon pool in the order

497   of ~ 80-400 µg C L^{-1} (Table 1 and Table 2) with the percentage of TEP-C from TOC ranging between

498   0.08- 42 % and 11-32 % at LDA and LDB respectively (Table 1 and 2, taking into account spatial and

499   temporal differences). Thus, at LDB, surface TEP-C increased from 22 % at day 3 to 32 % of the TOC

500   content at day 5. Yet, for the same time period a 2-fold increase of TEP was measured at 200 m (11 %

501   to 21 %). These results reflect the bloom status at LDB. During bloom development; organic C and N

502   are incorporated to the cells and little biotic TEP production occurs while stationary growth (as long as

503   photosynthesis continues) stimulates TEP production (Berman-Frank and Dubinsky, 1999). When

504   mortality exceeds growth, the presence of large amounts of sticky TEP provide "hot spots" or

505   substrates for bacterial activity and facilitate aggregation of particles and enhanced sinking rates of

506   aggregates as previously observed for *Trichodesmium* (Bar-Zeev et al., 2013).

507   **3.4. Linking PCD-induced bloom demise to particulate C and N export**

508   Measurements of elevated rates metacaspase and caspase activities and changes in TEP

509   concentrations are not sufficient to link PCD and vertical export of organic matter as was previously

510   shown in laboratory cultures of *Trichodesmium* (Bar-Zeev et al., 2013). To see whether PCD-induced

511   mortality led to enhanced carbon flux at sea we now examined mass flux and specific evidence for

512   diazotrophic contributions from the drifting sediment traps (150, 330 and 520 m) at LDA and LDB

513   stations.

514   Mass flux was measured at LDA, increasing over time with maximum mass flux rates at the 150 m

515   trap with 123 dry weight (DW) m^{-2} d^{-1} on day 4. The highest mass flux was 40 and 27 DW m^{-2} d^{-1}

516   from the deeper sediment traps (325 and 500 m traps respectively). Particulate C (PC) and particulate

517   nitrogen (PN) showed similar trends as the mass flux. At LDA, PC varied between 3.2-30 mg sample^{-1}

518   and PN ranged from 0.3-3.17 mg sample^{-1} at the 150 m trap. At LDB PC varied from 1.6 to 6.1 mg

519   sample^{-1} and total particulate nitrogen ranged from 0.24 to 0.78 mg sample^{-1}. The total sediment flux

520   in the traps deployed at LDB ranged between 6.4 and 33.5 mg m^{-2} d^{-1}, with an average of 18.9 mg m^{-2}

521 d^{-1}. Excluding the deepest trap at 500 m where the high flux occurred at day 2, in the other traps the

522 highest export flux rate occurred at the last day at the station (day 5).

523   Analyses of the community found in the sediment traps, determined by qPCR from the

524 accumulated matter on day 5 at the station, confirmed that *Trichodesmium*, UCYN-B and het-1 were

525 the most abundant diazotrophs in the sediment traps at LDA and LDB stations (Caffin et al., 2017),

526 correlating to the dominant diazotrophs found at the surface of the ocean (measured on day 1).

527 *Trichodesmium* and *Richelia-Rhizosolenia* association (het-1) were the major contributors to

528 diazotroph export at LDA and LDB and UCYN-B and het-1 were the major contributors at LDC

529 (Caffin et al., 2017). At LDA *Trichodemsium* was found in the deeper depth traps with 2.6 x10^7 and

530 1.4x10^7 *nifH* copies L^{-1} at the 325 and 500 traps respectively. UCYN-B was detected in all traps with

531 the highest abundance in deeper depth traps with values of 4.2x10^6 and 2.8x10^6 *nifH* copies L^{-1} at the

532 325 and 500 m traps respectively. Het-1 was specifically found only in the 325 m trap with 2.0x10^7

533 *nifH* copies L^{-1} (Fig. 5a). In LDB traps, *Trichodesmium*, UCYN-B and het-1 were not detected at the

534 sediment trap at 150 m, rather in the deeper traps. At depth *Trichodesmium* counts were 9x10^5 at 325

535 m trap and 5x10^6 *nifH* copies L^{-1} for the 500 m trap (Fig. 5b). UCYN-B was 3.6x10^5 and 10x10^5 *nifH*

536 copies L^{-1} at 325 and 500 m traps respectively, and 6x10^6 and 1x10^7 *nifH* copies L^{-1} of het-1 (Fig. 5b).

537   While the average size of *Trichodesmium* and the association between *Rhizosolenia and Richelia*

538 is relatively large for microphytoplankton, the small unicellular UCYN-B (< 4 μm) were also found in

539 the sediment traps, including the deeper (500 m) traps. UCYN-B is often associated with larger

540 phytoplankton such as the diatom *Climacodium frauenfeldianum* (Bench et al., 2013) or in colonial

541 phenotypes (> 10 μm fraction) as has been observed in the northern tropical Pacific (ALOHA) (Foster

542 et al., 2013). The only other detection of UCYN-B in sediment traps was during the VAHINE

543 mesocsom experiment in the New Caledonian lagoon where sediment traps were deployed at

544 shallower depths (15 m) (Bonnet et al., 2015) and in high abundance in a floating sediment trap

545 deployed at 75 m for 24 h is the North Pacific Subtropical Gyre (Sohm et al., 2011). Thus our data

546 substantiates earlier conclusions that UCYN, which form large aggregates (increasing actual size and

547 sinking velocities), can efficiently contribute to export in oligotrophic systems (Bonnet et al., 2015).

548 Increase in aggregate size could also occur with depth, possibly due to the high concentrations of TEP

549 produced at the surface layer, sinking in the water column, providing a nutrient source and enhancing

550 aggregation (Berman-Frank et al., 2016) which could also increase in size with depth due to TEP.

551 While this process was previously shown during a mesocosem experiment (Bonnet et al., 2015), it is

552 now shown to be applicable also in the open-ocean system.

553   Sinking rates of aggregates in the water depends on many factors such as fluid viscosity, particle

554 source material, morphology, density, and other variable particle characteristics. Sinking velocities of

555 diatoms embedded in aggregates are generally fast (50-200 m d^{-1}) (Asper, 1987;Alldredge, 1998)

556 compared with those of individually sinking cells (1^{-10} m d^{-1}) (Culver and Smith, 1989) allowing

Biogeosciences

Open Access

Discussions

EGU

557   aggregated particles to sink out of the photic zone to depth. Assuming a sinking rate of

558   *Trichodesmium*-based aggregates of 150-200 m d^{-1} (Bar-Zeev et al., 2013), we would need to shift the

559   time frame by 1 day to see whether PCD measured from the surface waters is coupled with changes in

560   organic matter reflected in the 150 m sediment traps. Thus, at LDA, examining metacaspase activities

561   from the surface with mass flux and particulate matter obtained 24 h later yielded a significant positive

562   correlation between these two parameters (Fig. 5c).

563   LDA had the highest export fluxes and particulate matter found in its traps relative to LDB and

564   LDC. Diazotrophs contributed ~ 36 % to PC export to the 325 m trap at LDA, with *Trichodesmium*

565   comprising the bulk of diazotrophs (Caffin et al., 2017) In contrast, at LDB, we found lower flux rates

566   in the traps and lower organic material with *Trichodesmium* contributing the bulk of diazotroph

567   biomass at the 150 m trap. We believe that at LDB the decline phase began only halfway through our

568   sampling and thus the resulting export efficiency we obtained for the 5 days at station was relatively

569   low compared to the total amount of surface biomass. Moreover, considering export rates, and the

570   experimental time frame, most of the diazotrophic population may have been directly exported to the

571   traps only after we left the station (i.e. time frame > 5 days). This situation is different from the bloom

572   at LDA, where enhanced mortality, biomass deterioration, and bloom crash were initiated 1-2 weeks

573   before our arrival and sampling at the station. Thus, at LDA, elevated mass flux and higher

574   concentrations of organic matter were obtained from all three depths of the deployed traps.

575   **4.   Conclusion and implications**

576   Our specific objective in this study was to examine whether diazotroph mortality mediated by

577   PCD can lead to higher fluxes of organic matter sinking to depth. The OUTPACE cruise provided this

578   opportunity in two out of three long-duration (5 day) stations where large surface blooms of

579   diazotrophs principally comprised of *Trichodesmium*, UCYN-B and diatom-diazotroph associations

580   *Rhizosolenia* and *Richelia* were encountered. Probing the biomass for characteristic indices of PCD

581   demonstrated high metacaspase activities, positively and significantly correlated to caspase-like

582   activities at both LDA and LDB, and reported here for the first time (metacaspase activity) in oceanic

583   populations of *Richelia* and *Trichodesmium*. We further show that TEP, facilitating aggregation of

584   biomass and enhancing sinking velocities, was high at both locations and changed with depth as

585   biomass declined. Moreover, we were able to specifically link for the first time in the open ocean

586   between blooms mediated by PCD and vertical fluxes through the deployment of sediment traps.

587   Yet, our results also delineate the natural variability of biological oceanic populations. The two

588   stations, LDA and LDB were characterized by biomass at physiologically different stages with the

589   biomass at LDA displaying more pronounced mortality that had begun prior to our arrival at station. In

590   contrast, satellite data indicated that at LDB, the surface *Trichodesmium* bloom was sustained for at

591   least a month prior to arrival and remained high for the first 3 days of our sampling before declining

592   by 40 % at day 5. As sediment trap material was examined during a short time frame of only 5 days at

17

593   each LD station, we assume that a proportion of the sinking diazotrophs and organic matter were not

594   yet collected in the traps and had either sunk before trap deployment or would sink after we left the

595   stations. Thus, these different historical conditions which influence physiological status at each

596   location also impacted the specific results we obtained and emphasized a-priori the importance of

597   comprehensive spatial and temporal sampling that would facilitate a more holistic understanding of

598   the dynamics and consequences of bloom formation and fate in the oceans.

599

600   **Author contributions**

601   IBF, DS, and SB conceived and designed the investigation linking PCD to vertical flux within the

602   OUTPACE project. NB, MS, AC, MPP, NL CD and RAF participated, collected and performed analyses

603   of samples, DS analysed samples and data. DS and IBF wrote the manuscript with contributions from

604   all co-authors.

605

606   **Acknowledgments**

629 **References**

630 Alldredge, A.: The carbon, nitrogen and mass content of marine snow as a function of aggregate size,
631 Deep Sea Research Part I: Oceanographic Research Papers, 45, 529-541, 1998.

632 Aminot, A., and Kérouel, R.: Dosage automatique des nutriments dans les eaux marines: méthodes en
633 flux continu, Editions Quae, 2007.

634 Asper, V. L.: Measuring the flux and sinking speed of marine snow aggregates, Deep Sea Research
635 Part A. Oceanographic Research Papers, 34, 1-17, 1987.

636 Asplund-Samuelsson, J., Bergman, B., and Larsson, J.: Prokaryotic caspase homologs: phylogenetic
637 patterns and functional characteristics reveal considerable diversity, PLoS One, 7, e49888, 2012.

638 Asplund-Samuelsson, J.: The art of destruction: revealing the proteolytic capacity of bacterial caspase
639 homologs, Molecular microbiology, 98, 1-6, 2015.

640 Bar-Zeev, E., Berman-Frank, I., Liberman, B., Rahav, E., Passow, U., and Berman, T.: Transparent
641 exopolymer particles: Potential agents for organic fouling and biofilm formation in desalination and
642 water treatment plants, Desalination and Water Treatment, 3, 136-142, 2009.

643 Bar-Zeev, E., Avishay, I., Bidle, K. D., and Berman-Frank, I.: Programmed cell death in the marine
644 cyanobacterium *Trichodesmium* mediates carbon and nitrogen export, The ISME journal, 7, 2340-
645 2348, 2013.

646 Bench, S. R., Heller, P., Frank, I., Arciniega, M., Shilova, I. N., and Zehr, J. P.: Whole genome
647 comparison of six *Crocosphaera watsonii* strains with differing phenotypes, Journal of phycology, 49,
648 786-801, 2013.

649 Bergman, B., Sandh, G., Lin, S., Larsson, J., and Carpenter, E. J.: *Trichodesmium* - a widespread
650 marine cyanobacterium with unusual nitrogen fixation properties, FEMS Microbiol Rev, 1-17, 2012.

651 Berman-Frank, I., and Dubinsky, Z.: Balanced growth in aquatic plants: Myth or reality?
652 Phytoplankton use the imbalance between carbon assimilation and biomass production to their
653 strategic advantage, Bioscience, 49, 29-37, 1999.

654 Berman-Frank, I., Bidle, K., Haramaty, L., and Falkowski, P.: The demise of the marine
655 cyanobacterium, *Trichodesmium* spp., via an autocatalyzed cell death pathway, Limnol. Oceanogr.,
656 49, 997-1005, 2004.

657 Berman-Frank, I., Rosenberg, G., Levitan, O., Haramaty, L., and Mari, X.: Coupling between
658 autocatalytic cell death and transparent exopolymeric particle production in the marine
659 cyanobacterium *Trichodesmium*, Environmental Microbiology, 9, 1415-1422, 10.1111/j.1462-
660 2920.2007.01257.x, 2007.

661 Berman-Frank, I., Spungin, D., Rahav, E., Wambeke, F. V., Turk-Kubo, K., and Moutin, T.:
662 Dynamics of transparent exopolymer particles (TEP) during the VAHINE mesocosm experiment in
663 the New Caledonian lagoon, Biogeosciences, 13, 3793-3805, 2016.

664 Bidle, K. D., and Bender, S. J.: Iron starvation and culture age activate metacaspases and programmed
665 cell death in the marine diatom *Thalassiosira pseudonana*, Eukaryotic Cell, 7, 223-236,
666 10.1128/ec.00296-07, 2008.

667 Bidle, K. D.: The molecular ecophysiology of programmed cell death in marine phytoplankton,
668 Annual review of marine science, 7, 341-375, 2015.

669   Bonnet, S., Guieu, U., Chiaverini, J., Ras, J., and Stock, A.: Effect of atmospheric nutrients on the
670   autotrophic communities in a low nutrient, low chlorophyll system, Limnology and Oceanography, 50,
671   1810-1819, 2005.

672   Bonnet, S., Berthelot, H., Turk-Kubo, K., Fawcett, S., Rahav, E., l'Helguen, S., and Berman-Frank, I.:
673   Dynamics of N_2 fixation and fate of diazotroph-derived nitrogen in a low nutrient low chlorophyll
674   ecosystem: results from the VAHINE mesocosm experiment (New Caledonia), Biogeosciences, 12,
675   19579-19626, doi:10.5194/bgd-12-19579-2015, 2015.

676   Bonnet, S., Caffin, M., Berthelot, H., Grosso, O., Guieu, C., and Moutin, T.: Contribution of dissolved
677   and particulate fractions to the Hot Spot of N_2 fixation in the Western Tropical South Pacific Ocean
678   (OUTPACE cruise), Biogeosciences, in reveiw, 2017a.

679   Bonnet, S., Caffin, M., Berthelot, H., and Moutin, T.: Hot spot of N_2 fixation in the western tropical
680   South Pacific pleads for a spatial decoupling between N_2 fixation and denitrification, Proceedings of
681   the National Academy of Sciences, 114, E2800-E2801, 10.1073/pnas.1619514114, 2017b.

682   Brussaard, C. P. D., Mari, X., Van Bleijswijk, J. D. L., and Veldhuis, M. J. W.: A mesocosm study of
683   Phaeocystis globosa (Prymnesiophyceae) population dynamics - II. Significance for the microbial
684   community, Harmful Algae, 4, 875-893, 2005.

685   Caffin, M., Moutin, T., Foster, R. A., Bouruet-Aubertot, P., Doglioli, A. M., Berthelot, H., Grosso, O.,
686   Helias-Nunige, S., Leblond, N., and Gimenez, A.: Nitrogen budgets following a Lagrangian strategy
687   in the Western Tropical South Pacific Ocean: the prominent role of N_2 fixation (OUTPACE cruise),
688   Biogeosciences In review, 2017.

689   Capone, D. G., Zehr, J. P., Paerl, H. W., Bergman, B., and Carpenter, E. J.: *Trichodesmium*, a globally
690   significant marine cyanobacterium, Science, 276, 1221-1229, 1997.

691   Carpenter, E. J., Subramaniam, A., and Capone, D. G.: Biomass and primary productivity of the
692   cyanobacterium *Trichodesmium* spp. in the tropical N Atlantic ocean, Deep-Sea Research Part I-
693   Oceanographic Research Papers, 51, 173-203, 10.1016/j.dsr.2003.10.006, 2004.

694   Cauwet, G.: HTCO method for dissolved organic carbon analysis in seawater: influence of catalyst on
695   blank estimation, Marine Chemistry, 47, 55-64, 1994.

696   Church, M. J., Jenkins, B. D., Karl, D. M., and Zehr, J. P.: Vertical distributions of nitrogen-fixing
697   phylotypes at Stn ALOHA in the oligotrophic North Pacific Ocean, Aquatic Microbial Ecology, 38, 3-
698   14, 2005.

699   Culver, M. E., and Smith, W. O.: Effects of environmental variation on sinking rates of marine
700   phytoplankton, Journal of phycology, 25, 262-270, 1989.

701   de Verneil, A., Rousselet, L., Doglioli, A. M., Petrenko, A. A., and Moutin, T.: The fate of a southwest
702   Pacific bloom: gauging the impact of submesoscale vs. mesoscale circulation on biological gradients
703   in the subtropics, Biogeosciences, 14, 3471, 2017.

704   Dupouy, C., Neveux, J., Subramaniam, A., Mulholland, M. R., Montoya, J. P., Campbell, L., Capone,
705   D. G., and Carpenter, E. J.: Satellite captures *Trichodesmium* blooms in the SouthWestern Tropical
706   Pacific., EOS, Trans American Geophysical Union,, 81, 13-16, 2000.

707   Dupouy, C., Benielli-Gary, D., Neveux, J., Dandonneau, Y., and Westberry, T. K.: An algorithm for
708   detecting *Trichodesmium* surface blooms in the South Western Tropical Pacific, Biogeosciences, 8,
709   3631-3647, 10.5194/bg-8-3631-2011, 2011.

710   Engel, A., Goldthwait, S., Passow, U., and Alldredge, A.: Temporal decoupling of carbon and nitrogen
711   dynamics in a mesocosm diatom bloom, Limnology and Oceanography, 47, 3, 753-761, 2002.

712   Engel, A.: Distribution of transparent exopolymer particles (TEP) in the northeast Atlantic Ocean and
713   their potential significance for aggregation processes, Deep-Sea Research Part I-Oceanographic
714   Research Papers, 51, 83-92, 2004.

715   Foster, R. A., Subramaniam, A., Mahaffey, C., Carpenter, E. J., Capone, D. G., and Zehr, J. P.:
716   Influence of the Amazon River plume on distributions of free-living and symbiotic cyanobacteria in
717   the western tropical north Atlantic Ocean, Limnology and Oceanography, 52, 517-532, 2007.

718   Foster, R. A., Sztejrenszus, S., and Kuypers, M. M.: Measuring carbon and N_2 fixation in field
719   populations of colonial and free-living unicellular cyanobacteria using nanometer-scale secondary ion
720   mass spectrometry1, Journal of phycology, 49, 502-516, 2013.

721   Fukao, T., Kimoto, K., and Kotani, Y.: Production of transparent exopolymer particles by four diatom
722   species, Fisheries science, 76, 755-760, 2010.

723   Garcia, N., Raimbault, P., and Sandroni, V.: Seasonal nitrogen fixation and primary production in the
724   Southwest Pacific: nanoplankton diazotrophy and transfer of nitrogen to picoplankton organisms,
725   Marine Ecology Progress Series, 343, 25-33, 2007.

726   Hewson, I., Govil, S. R., Capone, D. G., Carpenter, E. J., and Fuhrman, J. A.: Evidence of
727   *Trichodesmium* viral lysis and potential significance for biogeochemical cycling in the oligotrophic
728   ocean, Aquatic Microbial Ecology, 36, 1-8, 2004.

729   Jiang, X. D., Lonsdale, D. J., and Gobler, C. J.: Grazers and vitamins shape chain formation in a
730   bloom-forming dinoflagellate, *Cochlodinium polykrikoides*, Oecologia, 164, 455-464,
731   10.1007/s00442-010-1695-0, 2010.

732   Kerbrat, A. S., Amzil, Z., Pawlowiez, R., Golubic, S., Sibat, M., Darius, H. T., Chinain, M., and
733   Laurent, D.: First evidence of palytoxin and 42-hydroxy-palytoxin in the marine cyanobacterium
734   *Trichodesmium*, Marine drugs, 9, 543-560, 2011.

735   Klemenčič, M., Novinec, M., and Dolinar, M.: Orthocaspases are proteolytically active prokaryotic
736   caspase homologues: the case of *Microcystis aeruginosa*, Molecular microbiology, 98, 142-150, 2015.

737   Le Bouteiller, A., Blanchot, J., and Rodier, M.: Size distribution patterns of phytoplankton in the
738   western Pacific: towards a generalization for the tropical open ocean, Deep Sea Research Part A.
739   Oceanographic Research Papers, 39, 805-823, 1992.

740   Minina, E., Coll, N., Tuominen, H., and Bozhkov, P.: Metacaspases versus caspases in development
741   and cell fate regulation, Cell Death and Differentiation, 24, 1314, 2017.

742   Moisander, P. H., Beinart, R. A., Voss, M., and Zehr, J. P.: Diversity and abundance of diazotrophic
743   microorganisms in the South China Sea during intermonsoon, Isme Journal, 2, 954-967,
744   10.1038/ismej.2008.51, 2008.

745   Moisander, P. H., Beinart, R. A., Hewson, I, White, A. E., Johnson, K. S., Carlson, C. A., Montoya, J.
746   P., and Zehr, J. P.: Unicellular Cyanobacterial Distributions Broaden the Oceanic N-2 Fixation
747   Domain, Science, 327, 1512-1514, 10.1126/science.1185468, 2010.

748   Moutin, T., Doglioli, A. M., De Verneil, A., and Bonnet, S.: Preface: The Oligotrophy to the UlTra-
749   oligotrophy PACific Experiment (OUTPACE cruise, 18 February to 3 April 2015), Biogeosciences,
750   14, 3207, 2017.

751 O'Neil, J. M., and Roman, M. R.: Ingestion of the Cyanobacterium *Trichodesmium* spp by Pelagic
752 Harpacticoid Copepods Macrosetella, Miracia and Oculostella, Hydrobiologia, 293, 235-240, 1994.

753 O'Neil, J. M.: The colonial cyanobacterium *Trichodesmium* as a physical and nutritional substrate for
754 the harpacticoid copepod *Macrosetella gracilis*, Journal of Plankton Research, 20, 43-59, 1998.

755 Ohki, K.: A possible role of temperate phage in the regulation of Trichodesmium biomass, Bulletin de
756 l'institute oceanographique, Monaco, 19, 287-291, 1999.

757 Passow, U., and Alldredge, A. L.: A dye binding assay for the spectrophotometeric measurement of
758 transparent exopolymer particles (TEP), Limnol. & Oceanogr, 40, 1326-1335, 1995.

759 Passow, U.: Transparent exopolymer particles (TEP) in aquatic environments, Progress in
760 Oceanography, 55, 287-333, 2002.

761 Rodier, M., and Le Borgne, R.: Population dynamics and environmental conditions affecting
762 *Trichodesmium* spp. (filamentous cyanobacteria) blooms in the south-west lagoon of New Caledonia,
763 Journal of Experimental Marine Biology and Ecology, 358, 20-32, 10.1016/j.jembe.2008.01.016,
764 2008.

765 Rodier, M., and Le Borgne, R.: Population and trophic dynamics of *Trichodesmium thiebautii* in the
766 SE lagoon of New Caledonia. Comparison with *T. erythraeum* in the SW lagoon, Marine Pollution
767 Bulletin, 61(7-12), 349-359, 10.1016/j.marpolbul.2010.06.018, 2010.

768 Short, S. M., Jenkins, B. D., and Zehr, J. P.: Spatial and temporal distribution of two diazotrophic
769 bacteria in the Chesapeake Bay, Applied and Environmental Microbiology, 70, 2186-2192, 2004.

770 Sohm, J. A., Edwards, B. R., Wilson, B. G., and Webb, E. A.: Constitutive extracellular
771 polysaccharide (EPS) production by specific isolates of Crocosphaera watsonii, Frontiers in
772 microbiology, 2, 2011.

773 Spungin, D., Pfreundt, U., Berthelot, H., Bonnet, S., AlRoumi, D., Natale, F., Hess, W. R., Bidle, K.
774 D., and Berman-Frank, I.: Mechanisms of *Trichodesmium* demise within the New Caledonian lagoon
775 during the VAHINE mesocosm experiment, Biogeosciences, 13, 4187-4203, 2016.

776 Stenegren, M., Caputo, A., Berg, C., Bonnet, S., and Foster, R. A.: Distribution and drivers of
777 symbiotic and free-living diazotrophic cyanobacteria in the Western Tropical South Pacific, Biosci.
778 Discuss, 1-47, 2017.

779 Sugimura, Y., and Suzuki, Y.: A high-temperature catalytic oxidation method for the determination of
780 non-volatile dissolved organic carbon in seawater by direct injection of a liquid sample, Marine
781 Chemistry, 24, 105-131, 1988.

782 Tenorio, M., Dupouy C., Rodier, M., and Neveux, J.: *Trichodesmium* and other Filamentous
783 Cyanobacteria in New Caledonian waters (South West Tropical Pacific) during an El Niño Episode,
784 Aquatic Microbial Ecology, in review.

785 Thompson, A. W., Foster, R. A., Krupke, A., Carter, B. J., Musat, N., Vaulot, D., Kuypers, M. M., and
786 Zehr, J. P.: Unicellular cyanobacterium symbiotic with a single-celled eukaryotic alga, Science, 337,
787 1546-1550, 2012.

788 Tsiatsiani, L., Van Breusegem, F., Gallois, P., Zavialov, A., Lam, E., and Bozhkov, P.: Metacaspases,
789 Cell Death & Differentiation, 18, 1279-1288, 2011.

Biogeosciences

Open Access

EGU

Discussions

790 Turk-Kubo, K. A., Frank, I. E., Hogan, M. E., Desnues, A., Bonnet, S., and Zehr, J. P.: Diazotroph
791 community succession during the VAHINE mesocosm experiment (New Caledonia lagoon),
792 Biogeosciences, 12, 7435-7452, 2015.

793 Urbani, R., Magaletti, E., Sist, P., and Cicero, A. M.: Extracellular carbohydrates released by the
794 marine diatoms *Cylindrotheca closterium*, *Thalassiosira pseudonana* and *Skeletonema costatum*:
795 Effect of P-depletion and growth status, Science of the Total Environment, 353, 300-306, 2005.

796 Verdugo, P., and Santschi, P. H.: Polymer dynamics of DOC networks and gel formation in seawater,
797 Deep Sea Research Part II: Topical Studies in Oceanography, 57, 1486-1493, 2010.

798

799

800

801

802

803

804

805

806

807

808

809

810

811

812

813

814

815

816

817

818

819

820   **Figure legends**

821

822   **Figure 1-** Temporal dynamics of surface chlorophyll-a concentrations in the long duration (LD)

823   stations **(a)** LDA **(b)** LDB and **(c)** LDC station. Chlorophyll a was measured over 5 days at each

824   station (marked in gray). Satellite data of daily surface chlorophyll a (mg m^{-3}) around the long duration

825   stations of OUTPACE was used to predict changes in photosynthetic biomass before and after our

826   measurements at the station (marked as dashed lines). Satellite data movies are added as

827   supplementary data (Supplementary videos S1, S2, S3). Chlorophyll a profiles in **(d)** LDA **(e)** LDB

828   and **(f)** LDC. Measurements of Chl *a* were taken on days 1 (black dot), 3 (white triangle) and 5 (grey

829   square) at the LDB station at 5 depths between surface and 200 m depths.

830
831   **Figure 2- (a-d)** Microscopic images of *Trichodesmium* from LDA and LDB. Observations of poor cell

832   integrity were reported for collected samples, with filaments at various stages of degradation and

833   colony under possible stress. **(e)** Confocal and **(d)** processed IMARIS images of *Rhizosolenia-Richelia*

834   symbioses (het-1) at 6m (75 % surface incidence). Green fluorescence indicate the chloroplast of the

835   diatoms, and red fluorescence are the *Richelia* filaments; Microscopic observations indicate that near

836   the surface *Rhizosolenia* populations were already showing signs of decay since the silicified cell-wall

837   frustules were broken and free filaments of *Richelia* were observed. Images by Andrea Caputo.

838

839   **Figure 3- PCD indices from LDA and LDB (a)** Caspase activity from LDA (pM hydrolyzed mg

840   protein^{-1} min^{-1}) assessed by cleavage of the canonical fluorogenic substrate, z-IETD-AFC. **(b)**

841   Metacaspase activity from LDA (pM hydrolyzed mg protein^{-1} min^{-1}) assessed by cleavage of the

842   canonical fluorogenic substrate, VRPR-AMC. **(c)** Relationship between caspase activity and

843   metacaspase activity from LDA (R^2=0.7, n=15, p<0.001). **(d)** Caspase activity rats in LDB station (pM

844   hydrolyzed mg protein^{-1} min^{-1}), **(e)** Metacaspase activity in LDB station (pmol hydrolyzed mg protein^{-1}

845   min^{-1}), **(f)** Relationship between caspase activity and metacaspase activity in LDB station (R^2=0.6,

846   n=15, p<0.001). Caspase and metacaspase activates at LDA and LDB stations were measured on days:

847   1(black dot), 3 (white triangle) and 5 (grey square) between surface and 200 m. Error bars represent ±

848   1 standard deviation (n=3).

849

850   **Figure 4- (a)** Depth profiles of TEP concentrations (µg GX L^{-1}) at LDB station. Measurements were

851   taken on days 1, 3 and 5 at the station at surface-200 m depths. **(b)** The relationships between the

852   concentration of transparent exopolymeric particles (TEP), (µg GX L^{-1}) and dissolved inorganic

853   phosphorus DIP (µmol L^{-1}) for days 1, 3 and 5 at the LDB station (R^2=0.5, n=15, p<0.001).

854   Relationships between the concentration of transparent exopolymeric particles (TEP), (µg GX L^{-1}) and

855   **(c)** metacaspase activity (pmol hydrolyzed mg protein^{-1} min^{-1}) for days 1, 3 and 5 at the LDB (R^2=0.4,

856   n=15, p<0.05); **(d)** and with dissolved organic carbon (DOC), (µM) for days 1, 3 and 5 at the LDB

857   station (R^2=0.58, n=15, p<0.001) **(e)** and with particulate organic carbon (POC) (μM) for days 1, 3 and

858   5 at the LDB station (R^2=0.85, n=8, p<0.001 for day 1 and R^2=0.97, n=5 p<0.01 for day 3and 5) **(f)**

859   and with total organic carbon (TOC) (μM) for days 1, 3 and 5 at the LDB station (R^2=0.65, n=15,

860   p<0.0001). Measurements were taken on days 1 (black dot), 3 (white triangle) and 5 (grey square) at

861   LDB at 5 depths between surface and 200 m depths. Error bars for TEP represent ± 1 standard

862   deviation (n=3)**.**

863

864   **Figure 5- (a)** Diazotrophic abundance (*nifH* copies L^{-1}) of *Trichodesmium* (dark grey bars); UCYN-B

865   (white bars); and het-1 (light grey bars) recovered in sediment traps at the long duration stations **(A)**

866   Diazotrophic abundance (*nifH* copies L^{-1}) observed in the traps at LDA station **(b)** Diazotrophic

867   abundance (*nifH* copies L^{-1}) observed in the traps at LDB station. Abundance was measured from the

868   accumulated material on day 5 at each station. Sediment traps were deployed at the LD station at 150

869   m, 325 m, and 500 m. Error bars represent ± 1 standard deviation (n=3). **(c)** Relationship between

870   metacaspase activity (pmol hydrolyzed mg protein^{-1} min^{-1}) measured at the surface waters of LDA

871   station and mass flux rates (mg m^2 h^{-1}) (green circle), particulate carbon (PC, mg sample^{-1}) (green

872   triangle) and particulate nitrogen (PN, mg sample^{-1}) (green square) measured in the sediment trap

873   deployed at 150 m. A 1-day shift between metacaspase activities at the surface showed a significant

874   positive correlation with mass flux and particulate matter obtained in the sediment trap at LDA station

875   at 150 m.

876

877

878

879

880

881

882

883

884

885

886

887

888

889

890 **Table 1**- Temporal changes in the relative composition (w/w) and distribution of TEP, TEP-C and
891 organic carbon and nitrogen fractions within the water column during days 1,3 and 5 in the LDA
892 station at different depth ranging between surface (10 m) to 200 m.
893

Day at LDA station	Depth (m)	TEP (µg GX L^{-1})	TEP-C	%TEP-C	POC (µM)	TOC (µM)	POC/PON
1	200	296±135	186.5	27.2	3.04	57.2	5
	150	ND	ND	ND	3.18	61.1	13
	70	87±17	54.8	6.7	2.93	68.7	11
	50	562±7	354.3	41.9	2.47	70.5	13
	10	241±40	152.3	14.5	9.21	87.4	8
3	200	191±13	120.9	18.6	1.29	54.2	27
	150	144±54	91.2	12.9	2.22	59.0	22
	80	263	166.1	20.5	4.62	67.5	15
	10	126±2	79.6	8.3	3.60	79.7	12
5	200	200	126	21.3	2.84	54.2	236
	150	220	138.6	18.0	2.72	58.2	7
	80	146	92.2	12.1	4.91	63.3	8
	50	348±60	219.5	26.8	3.33	68.3	6
	10	ND	ND	ND	5.80	83.7	7

894
895
896
897 **Table 2-** Temporal changes in the relative composition (w/w) and distribution of TEP, TEP-C and
898 organic carbon and nitrogen fractions within the water column during days 1,3 and 5 in the LDB
899 station at different depth ranging between surface (7 m) to 200 m.
900

| Day at LDB station	Depth (m)	TEP (µg GX L^{-1})	TEP-C	%TEP-C	POC (µM)	TOC (µM)	POC/PON
1	7	408±36	257.1	23.4	8.95	91.5	6.0
	35	279±86	175.9	17.0	5.86	86.0	9.1
	100	214±67	134.7	16.8	ND	66.7	ND
	150	145±34	91.5	12.3	3.79	61.9	11.2
	200	244±113	153.7	20.3	7.61	63.2	9.8
3	7	402±12	253.1	22.5	8.88	93.9	6.9
	35	193±48	121.8	12.6	3.07	80.3	8.2
	100	163±33	102.4	12.6	ND	67.8	ND
	150	145±34	91.6	12.0	1.91	63.8	7.4
	200	127±79	80.2	11.3	1.71	59.3	5.7
5	7	565±87	355.8	32.5	5.32	91.3	5.9
	70	294±53	185.2	20.1	2.21	76.7	6.1
	100	264±160	166.2	19.6	2.25	70.6	8.0
	150	224±51	140.8	15.9	1.53	73.9	5.1
	200	231±45	145.8	21.1	1.11	57.6	5.5

901
902 Abbreviations: TEP, transparent exopolymeric particle; TEP-C, TEP carbon; POC, particulate organic
903 C; TOC, total organic C; ND- no data.
904

905
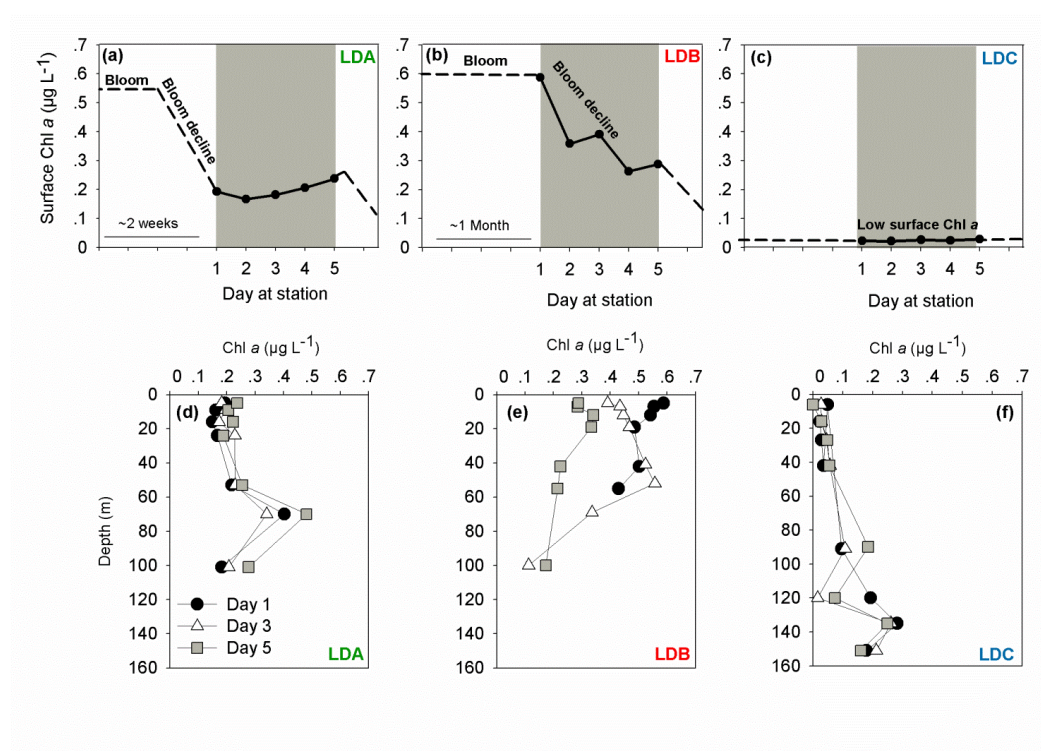
Figures

Figure 1

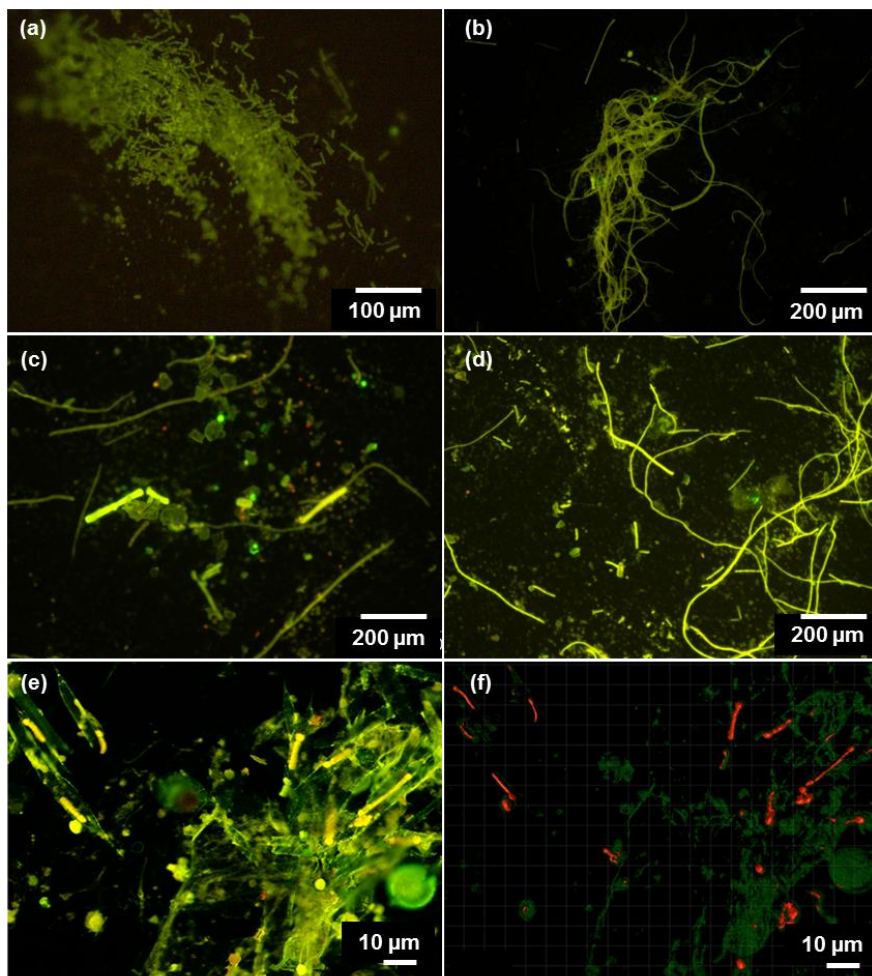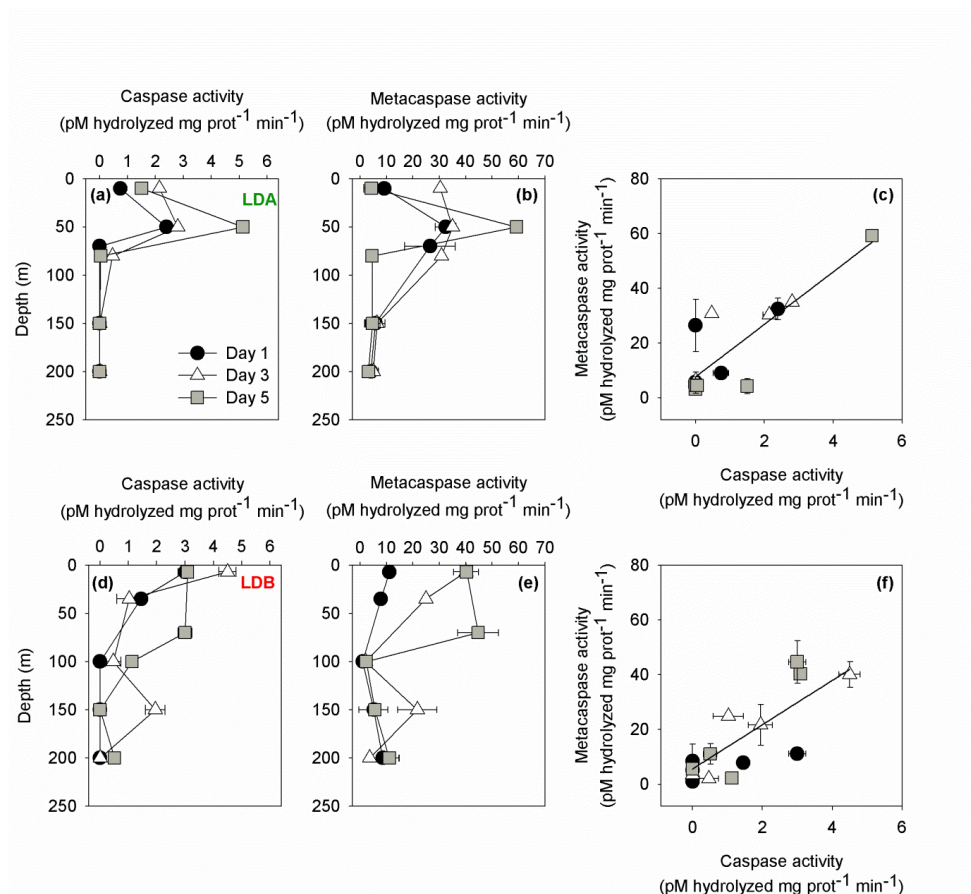915 **Figure 2**

916

917

918

919

920

921   **Figure 3**

922

923

924

925

926

927
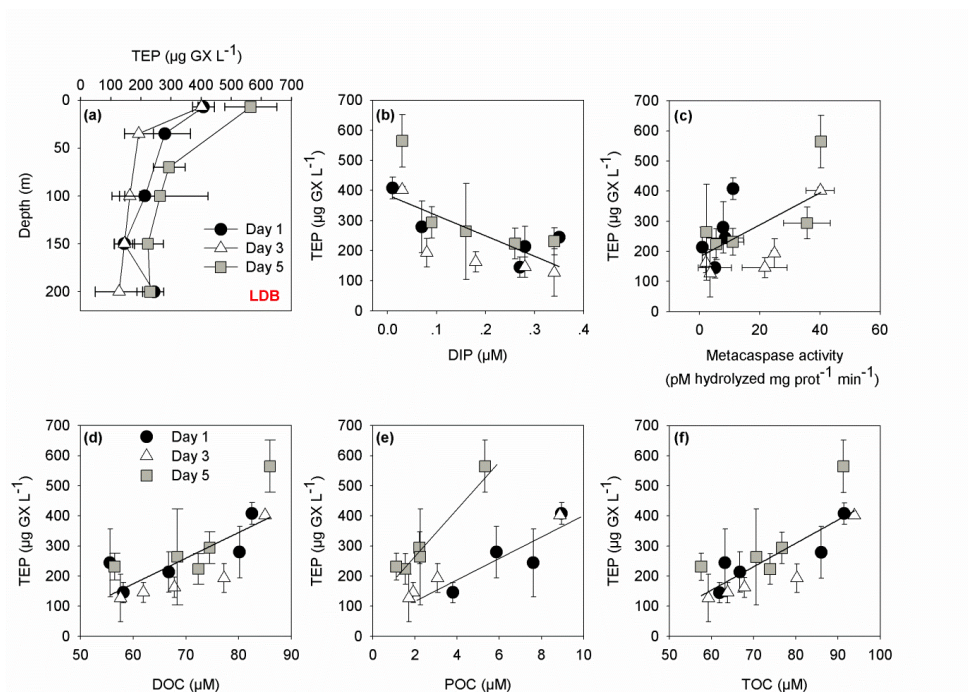
928

929 **Figure 4**

936 **Figure 5**

937

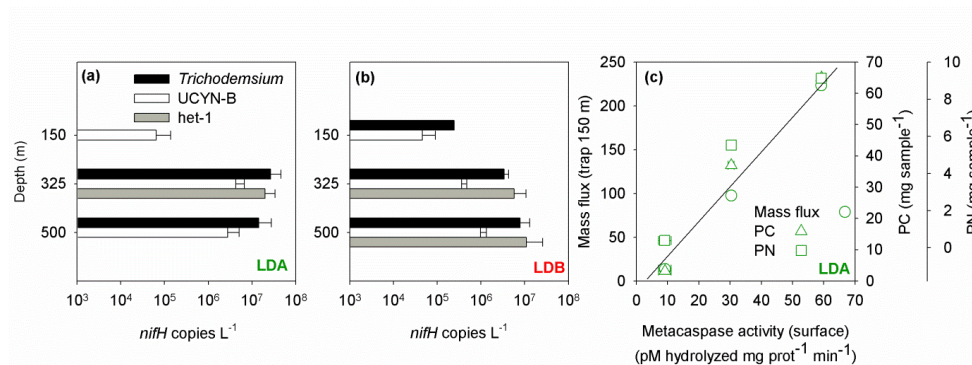938